J. Fluid Mech. (1982), *vol.* 117, *pp.* 443–455
Printed in Great Britain

Mathematical models for coating processes

By M. D. SAVAGE

Department of Applied Mathematical Studies,
University of Leeds, Leeds LS2 9JT, England

(Received 13 October 1980 and in revised form 29 July 1981)

The flow is considered of a Newtonian fluid, of viscosity η and surface tension T, in the narrow gap between a pair of rollers of radii R_1 and R_2, whose peripheral speeds are constant and equal to U_1 and U_2 respectively. The objective is to determine the coating thickness h_1^∞ on the upper roller as a function of the non-dimensional parameters H_0/R, $\eta U/T$ and U_1/U_2, where H_0 is the minimum gap thickness, $U = \frac{1}{2}(U_1+U_2)$, and $2R^{-1} = R_1^{-1}+R_2^{-1}$.

Using lubrication theory to provide an adequate description of the fluid flow, two mathematical models are derived whose essential difference lies in the specification of the boundary conditions. In the separation model it is assumed that the pressure distribution will terminate at a position which is both a stagnation point and a point of separation, whereas the Reynolds model incorporates the classical Reynolds conditions. In each case, theoretical predictions for the non-dimensional coating thickness, h_1^∞/H_0 as a function of U_1/U_2 are found to compare well with experiment. However, theory does suggest that the two models are applicable to different and complementary regions of parameter space, and hence together they may form a basis for further investigations into the various features of coating processes.

1. Introduction

Coating processes arise in a variety of contexts including the tin-plate, printing-ink, photographic, and paint industries. Generally they involve a pair of rollers of radii R_1 and R_2, as shown in figure 1, moving with peripheral speeds U_1 and U_2. Fluid is picked up from a reservoir by the lower roller; it passes through a narrow gap of minimum thickness H_0 and on emerging splits into two uniform layers of thickness h_1^∞ and h_2^∞ attached to the upper and lower rollers respectively. It is the layer on the upper roller that is used for coating and therefore one seeks to determine the way in which its thickness depends upon the system parameters.

Greener & Middleman (1975) analysed the symmetric problem in which the roller speeds are equal, $U_1 = U_2 = U$. Their model is based on the assumption that the fluid film extends over a semi-infinite domain terminating at a fluid–air interface where there is a stagnation point and where symmetry considerations imply that the gradient of velocity is zero; $\partial u/\partial z = 0$. Since the uniform layers attached to each roller have the same thickness, $h_1^\infty = h_2^\infty = h^\infty$, Greener & Middleman proceeded to show how the film-thickness ratio h^∞/H_0 varied with β, the modified capillary number defined by $\beta = (T/\eta U)(H_0/R)^{\frac{1}{2}}$.

The principal objective in this paper is to extend the work of Greener & Middleman to the general coating situation, which involves rollers of arbitrary size and speed;

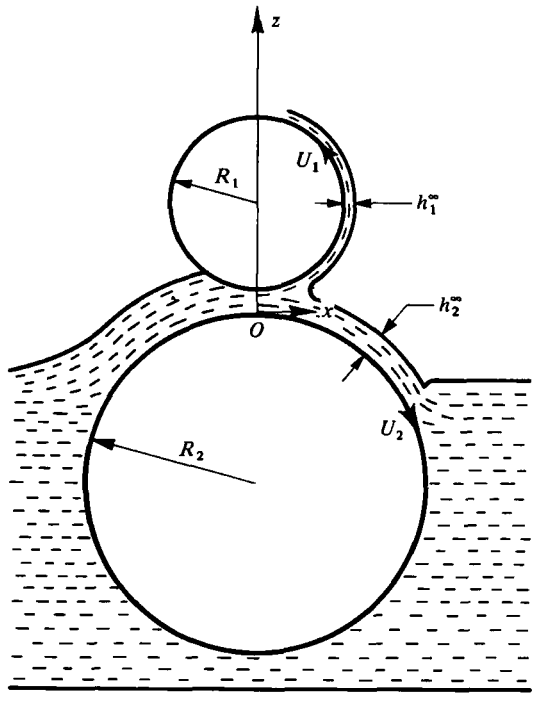

FIGURE 1. Viscous flow in the narrow gap between a pair of counter-rotating rollers.

$U_1 \neq U_2, U_1 > 0, U_2 > 0$. Following Greener & Middleman, lubrication theory is used to describe the flow of a Newtonian fluid in the semi-infinite domain shown in figure 1. It should be noted that the precise location of the fluid–air interface would require a two-dimensional analysis of the fluid flow in the vicinity of the interface, which is beyond the scope of the present paper. As a first step we shall present approximate yet simple boundary conditions which can be used to furnish useful results within the lubrication approximation. Consequently, two mathematical models are formulated for the pressure distribution, $P(x)$, over a semi-infinite domain.

In the *separation model* the pressure curve terminates where $u = \partial u/\partial z = 0$, which refers to a position that is both a stagnation point and a point of separation. That such a position may be located either on the interface or at the onset of a reverse flow region is discussed in § 2. Previously these conditions have been applied to two particular flows; to the symmetric coating problem mentioned earlier and to the flow between a cylinder and a flat substrate (Hopkins 1957), which from figure 1 corresponds to $R_1 = \infty, U_1 = 0$. In the former case the separation/stagnation point lies midway between the rollers, in the latter it is attached to the stationary surface. For the *Reynolds model* the classical Reynolds conditions $p = \partial p/\partial x = 0$ specify the termination of the pressure distribution.

A solution to the separation model yields the film-thickness ratio, $\lambda_1 = h_1^\infty/H_0$, as a function of speed ratio U_1/U_2, and modified capillary number β. However, in the region of practical interest, $\beta \ll 1$ and the variation of λ_1 with β is slight. Therefore if λ_1^L is the limiting value of λ_1 such that $\lambda_1 \to \lambda_1^L$ as $\beta \to 0$, then it is of interest to plot λ_1^L against U_1/U_2. For both the separation and Reynolds models it is found that

theoretical predictions are in good agreement with experimental data. Finally, the relative merits of the two models are discussed.

2. Mathematical Formulation

Figure 1 shows a cross-section of a two-roller system where the origin of (x, z)-coordinates is situated in the nip, such that the lower and upper roller surfaces are given by $z = 0$ and $z = h(x)$ respectively. The gap is assumed to be fully flooded upstream, so that fluid occupies the semi-infinite domain $-\infty \leqslant x \leqslant c$, where $x = c$ is the position of the fluid–air interface. At either extremity there arise regions of circulatory flow and free surfaces, for which a detailed analysis is beyond the scope of this paper. However, by following Pearson (1960), mathematical models can be formulated by making use of the lubrication approximation, which is assumed to be valid throughout the domain. Clearly, refinements to a basic model may be incorporated at a later stage.

The gap thickness is approximated by the equation

$$h(x) = H_0 + \frac{x^2}{2R_1} + \frac{x^2}{2R_2}, \tag{2.1}$$

such that if an average radius R is defined by

$$\frac{2}{R} = \frac{1}{R_1} + \frac{1}{R_2},$$

then (2.1) becomes

$$h(x) = H_0 + x^2/R. \tag{2.2}$$

Denoting the x-component of fluid velocity by $u(x, z)$ and introducing the usual lubrication assumptions that both gravity and inertia effects are negligible and $\partial/\partial z \gg \partial/\partial x$, then the Navier–Stokes equations reduce to

$$\frac{\partial p}{\partial x} = \eta \frac{\partial^2 u}{\partial z^2}, \quad \frac{\partial p}{\partial z} = 0, \tag{2.3), (2.4}$$

where p represents fluid pressure.

The solution of (2.3) and (2.4) subject to boundary conditions

$$u = U_1 \quad \text{on} \quad z = h(x), \quad u = U_2 \quad \text{on} \quad z = 0 \tag{2.5}$$

is

$$u(x, z) = \frac{1}{2\eta} \frac{\partial p}{\partial x} (z^2 - zh) + (U_1 - U_2) \frac{z}{h} + U_2. \tag{2.6}$$

For steady flows in which axial leakage is ignored, the flux Q of fluid past any station x is constant; hence continuity of flow yields

$$Q = \int_0^{h(x)} u \, dz = \text{const.} = U_1 h_1^\infty + U_2 h_2^\infty. \tag{2.7}$$

Substituting for $u(x, z)$ from (2.6) and performing the integration gives rise to

$$\frac{dp}{dx} = \frac{6\eta}{h^3(x)} [(U_1 + U_2) h(x) - 2Q], \tag{2.8}$$

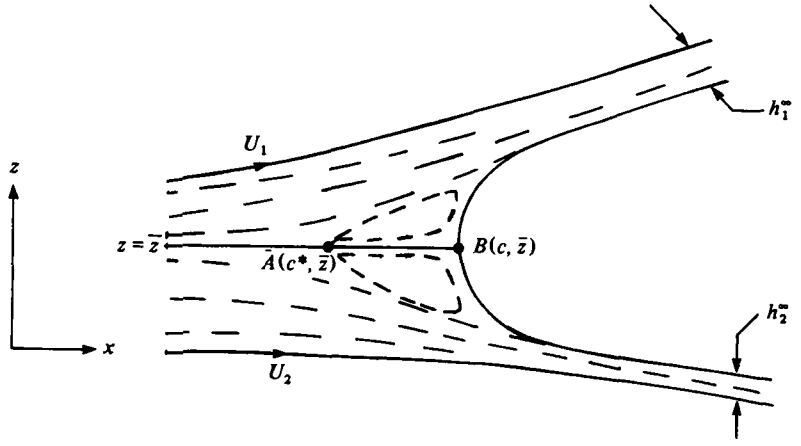

FIGURE 2. Flow near the downstream fluid–air interface showing the dividing streamline $z = \bar{z}$ which connects A, the onset of the reverse-flow region, to B the effective tip of the meniscus.

which can be solved, in principle, for $p(x)$, provided that two boundary conditions are specified, thus permitting the evaluation of Q and the constant of integration. Two conditions on pressure are

$$p(-\infty) = 0 \quad \text{(atmospheric pressure)},$$
$$p(c) = -T/r,$$

where r is the effective radius of curvature of the interface at its leading-edge. From figure 2 it is clear that an approximation to r, which can be achieved without solving the free-boundary problem is, given by

$$2r + h_1^\infty + h_2^\infty = h(c);$$

hence

$$r = \tfrac{1}{2}[h(c) - h_1^\infty - h_2^\infty]. \tag{2.9}$$

The formulation of a mathematical model is still incomplete, since the position $x = c$ remains unknown. A third condition is therefore required and it is precisely the specification of this third condition which distinguishes the separation model from the Reynolds model.

2.1. *Formulation of the separation model*

In this model the termination of the pressure distribution is achieved by means of one condition on pressure and two involving fluid speed;

$$p = -T/r, \tag{2.10}$$

$$u = 0, \quad \frac{\partial u}{\partial z} = 0. \tag{2.11}$$

Physically they refer to conditions at the onset of the reverse flow region, position $A(c^*, \bar{z})$ in figure 2, which is both a stagnation point and a point where the streamlines separate. In addition, it is necessary to regard the fluid–air interface as located downstream of A and assume that fluid pressure is constant throughout the reverse-flow region; $c^* \leqslant x \leqslant c$.

In passing, it is observed that the above conditions refer equally to the tip of the meniscus, position $B(c,\bar{z})$ in figure 2, which is also a stagnation/separation point. However, the velocity distribution $u(x,z)$, given by (2.6) and derived via the lubrication approximation, can in no way provide an adequate description of the two-dimensional flow in the reverse-flow region. Indeed it is readily seen that the application of (2.11) to (2.6) will yield only one (and not two) positions where velocity and velocity gradient are both zero. Hence it follows that the separation model can describe fluid flow only over the domain $-\infty < x \leqslant c^*$, and the termination of the domain is the onset of reverse flow and not the location of the meniscus.

Applying the above conditions to the velocity distribution (2.6) generates the following results:

$$\frac{\partial p}{\partial x}(c^*) = \frac{2\eta}{h^2(c^*)}[U_1^{\frac{1}{2}} + U_2^{\frac{1}{2}}]^2, \tag{2.12}$$

where

$$\bar{z} = \phi h(c^*),$$

$$\phi = \frac{U_2^{\frac{1}{2}}}{U_1^{\frac{1}{2}} + U_2^{\frac{1}{2}}}. \tag{2.13}$$

All that now remains is to determine the individual film thicknesses h_1^∞ and h_2^∞ by considering the fluid flow in the neighbourhood of the interface, as shown in figure 2. The dividing streamline $z = \bar{z}$ divides the volume of fluid that proceeds to flow around the upper roller in a uniform layer of thickness h_1^∞ from the volume that flows around the lower roller in a uniform layer of thickness h_2^∞. Continuity of flow requires that

$$U_1 h_1^\infty = \int_{\bar{z}}^{h(c^*)} u\,dz,$$

and therefore, after much algebra,

$$\frac{h_1^\infty}{h(c^*)} = \tfrac{1}{2}(1-\phi). \tag{2.14}$$

Similarly

$$U_2 h_2^\infty = \int_0^{\bar{z}} u\,dz,$$

$$\frac{h_2^\infty}{h(c^*)} = \tfrac{1}{2}\phi. \tag{2.15}$$

It is convenient to introduce non-dimensional film-thickness ratios λ_1, λ_2 defined by

$$\lambda_1 = \frac{h_1^\infty}{H_0}, \quad \lambda_2 = \frac{h_2^\infty}{H_0} \tag{2.16}$$

such that from expressions (2.14)–(2.16) all relevant quantities can be expressed in terms of λ_1 and ϕ;

(i) $$\lambda_2 = \lambda_1 \frac{\phi}{1-\phi},$$

(ii) $$\lambda_1 + \lambda_2 = \tfrac{1}{2}[1 + (c^*)^2/RH_0]$$

therefore

$$c^* = \left[\frac{3\lambda_1}{1-\phi} - 1\right]^{\frac{1}{2}} (RH_0)^{\frac{1}{2}}, \tag{2.17}$$

(iii)
$$\frac{r}{H_0} = \frac{1}{2}\left[\frac{h(c^*)}{H_0} - \lambda_1 - \lambda_2\right] = \frac{\lambda_1}{1-\phi}, \tag{2.18}$$

(iv)
$$Q = U_1 h_1^\infty + U_2 h_2^\infty = (U_1 + U_2) H_0 \lambda_1 \omega, \tag{2.19}$$

where

$$\omega = \frac{U_1^{\frac{3}{2}} + U_2^{\frac{3}{2}}}{U_1^{\frac{1}{2}}(U_1 + U_2)}. \tag{2.20}$$

Consequently the separation model may be formulated as follows: to solve, in $-\infty < x \leqslant c^*$,

$$\frac{dp}{dx} = 6\eta(U_1 + U_2)\frac{h(x) - 2\omega H_0 \lambda_1}{h^3(x)}, \tag{2.21}$$

subject to

$$p(-\infty) = 0, \tag{2.22}$$

$$p(c^*) = -T/r, \tag{2.23}$$

$$\frac{dp}{dx}(c^*) = \frac{2\eta}{h^2(c^*)}[U_1^{\frac{1}{2}} + U_2^{\frac{1}{2}}]^2. \tag{2.24}$$

By introducing further non-dimensional variables

$$x = (RH_0)^{\frac{1}{2}} X, \quad c^* = (RH_0)^{\frac{1}{2}} C^*,$$

it is found that

$$C^* = \left[\frac{3\lambda_1}{1-\phi} - 1\right]^{\frac{1}{2}}. \tag{2.25}$$

Hence the integration of (2.21) and the use of (2.22)–(2.25) yield the following equation:

$$-\frac{1}{12}(1-\phi)\beta = \lambda_1 \int_{-\infty}^{C^*} \frac{(1+X^2) - 2\omega\lambda_1}{(1+X^2)^3}\, dX, \tag{2.26}$$

where β is the modified capillary number defined by

$$\beta = \frac{T}{\eta U}\left(\frac{H_0}{R}\right)^{\frac{1}{2}}, \quad U = \tfrac{1}{2}(U_1 + U_2). \tag{2.27}$$

Equation (2.26) is a generalized form of that obtained by Greener & Middleman for the symmetric case when both rollers have equal speed. Results can be obtained giving λ_1 as a function of both U_1/U_2 and β.

2.2. *Limitations of the separation model*

The separation model, described by (2.21)–(2.24), can only apply to direct rolling. This follows since both ϕ and ω involve the square roots of the peripheral speeds U_1 and U_2, and it is therefore not feasible to reverse the sign of either the upper or lower roller speed for application to reverse rolling. Indeed, the character of the fluid flow in the vicinity of the fluid–air interface is significantly altered under conditions of reverse rolling and due account of this needs to be taken.

One limitation on the validity of the separation model under direct rolling conditions is seen by considering a typical pressure profile, figure 5, arising from the solution of (2.21)–(2.26). The overall shape of this curve, which features a sub-atmospheric pressure loop immediately upstream of the interface, has been experimentally verified by Smith (1975) under conditions of low pressure, i.e. pressures in the fluid that are not significantly larger than atmospheric pressure p_A. Taking $(RH_0)^{\frac{1}{2}}$ as a typical length scale for x, then

$$p(x) \sim O\left(\frac{\eta U}{H_0}\left(\frac{R}{H_0}\right)^{\frac{1}{2}}\right)$$

and therefore

$$\frac{\eta U}{H_0}\left(\frac{R}{H_0}\right)^{\frac{1}{2}} < p_A$$

will suffice. Hence

$$(T/H_0)\beta^{-1} < p_A \tag{2.28}$$

is the required criterion for low pressure generation, thus ensuring the validity of the separation model.

Under normal operating conditions, $\beta \ll 1$, and yet (2.28) will remain valid provided $(T/H_0)p_A^{-1} < \beta$, which is indeed the case in many coating processes. In fact the criterion (2.28) only fails when a coating process generates fluid pressures significantly higher than atmospheric pressure. The reason for this is as follows: as the magnitude of the positive pressures (above atmospheric) is increased, then correspondingly the magnitudes of the negative pressures are increased. Since there is a limit to the magnitude of the sub-atmospheric pressure which a fluid can sustain, then once this limit is reached the fluid film ruptures and the fluid–air interface is formed further upstream than would otherwise be the case. A typical pressure profile for high pressure generation ($\beta \to 0$) is shown in figure 6, where the appropriate conditions at rupture are well-known to lubrication engineers. They are the Reynolds conditions

$$p(c) = 0, \quad \frac{dp}{dx}(c) = 0. \tag{2.29), (2.30}$$

2.3. *Formulation of the Reynolds model*

In this section the objective is to formulate a mathematical model that is applicable to coating processes in that region of practical interest where $\beta \to 0$. The first problem is to justify the use of conditions (2.29) and (2.30) as $\beta \to 0$.

Pitts & Greiller (1961) and Savage (1977) have shown that a uniform fluid–air interface, $x = c$, will remain stable to small disturbances provided that at $x = c$,

$$\frac{dp}{dx} \leqslant \frac{d}{dx}(-T/r). \tag{2.31}$$

If, as in the separation model, dp/dx is assumed to be non-zero and $O(\mu U/H_0^2)$, then (2.31) is equivalent to

$$\beta \geqslant O(1). \tag{2.32}$$

Clearly, as $\beta \to 0$ the above inequality no longer holds, and as a consequence the interface cannot remain uniformly straight along the axis of the rollers. In fact the interface becomes ribbed such that the number of ribs per unit axial length varies

with $\eta U/T$ and H_0/R. Once ribs appear, giving rise to a wavy-like yet stationary interface, then the condition for stability is once again given by (2.31) provided that surface-tension pressures due to curvature in the (x, y)-plane are neglected. In the limit $\beta \to 0$, which essentially means that all surface-tension effects are negligible, then (2.31) and (2.23) reduce to

$$\frac{dp}{dx} = 0, \quad p = 0, \tag{2.33}$$

which are the familiar Reynolds conditions. The formulation of the Reynolds model is therefore as follows: to solve, in $-\infty < x \leqslant c$,

$$\frac{dp}{dx} = \frac{6\eta}{h^3(x)}\left[(U_1 + U_2)\, h(x) - 2U_1 h_1^\infty - 2U_2 h_2^\infty\right], \tag{2.34}$$

subject to

$$p(-\infty) = 0, \quad p(c) = 0, \quad \frac{dp}{dx}(c) = 0. \qquad (2.35), (2.36), (2.37)$$

The solution to the set of equations (2.34)–(2.37) for the pressure distribution $p(x)$ and the position of the interface $x = c$ is well-known: $p(x)$ is everywhere above atmospheric, and c takes a value of approximately $0{\cdot}46(RH_0)^{\frac{1}{2}}$. However, the Reynolds model, as described above, is incomplete – there are no additional conditions to determine ϕ ($\bar{z} = \phi h(c)$) which specifies the position of the dividing streamline immediately upstream of the interface as shown in figure 2. What is known is information concerning three special cases:

$$\left.\begin{aligned} &\text{(i)} \quad U_1 = U_2, \quad \phi = \tfrac{1}{2}, \quad \frac{h_1^\infty}{h(c)} = \frac{h_2^\infty}{h(c)} = \tfrac{1}{2}, \\ &\text{(ii)} \quad U_2 = 0, \quad \phi = 0, \quad \frac{h_1^\infty}{h(c)} = \tfrac{1}{2}, \quad h_2^\infty = 0, \\ &\text{(iii)} \quad U_1 = 0, \quad \phi = 1, \quad \frac{h_2^\infty}{h(c)} = \tfrac{1}{2}, \quad h_1^\infty = 0. \end{aligned}\right\} \tag{2.38}$$

In the absence of a more refined model that examines the fluid dynamics in the vicinity of and downstream of the interface then we must resort to speculative and intuitive arguments in order to derive a functional relationship between ϕ and the speeds (U_1, U_2). Any such functional relationship must satisfy (2.38), and many possibilities exist. One obvious candidate is the generalized form of equation (2.13) appearing in the separation model, namely

$$\phi = \frac{U_2^\alpha}{U_2^\alpha + U_1^\alpha}, \tag{2.39}$$

where α is a positive constant – as yet unknown.

We shall proceed by obtaining expressions for the two film thicknesses h_1^∞ and h_2^∞. Since $\bar{z} = \phi h(c)$ (figure 2), then continuity of flow for which $dp(c)/dx = 0$ yields

$$U_2 h_2^\infty = \int_0^{\phi h} u\, dz = U_2 \phi h + \tfrac{1}{2}(U_1 - U_2)\, \phi^2 h, \tag{2.40}$$

$$U_1 h_1^\infty = \int_{\phi h}^{h} u\, dz = U_2(1-\phi)\, h + \tfrac{1}{2}(U_1 - U_2)\,(1-\phi^2)\, h. \tag{2.41}$$

Hence

$$\frac{h_2^\infty}{h(c)} = \phi + \tfrac{1}{2}(S-1)\,\phi^2, \tag{2.42}$$

$$\frac{h_1^\infty}{h(c)} = \frac{(1-\phi)}{S} + \frac{1}{2}\left(1-\frac{1}{S}\right)(1-\phi^2), \tag{2.43}$$

where S is the speed ratio defined by $S = U_1/U_2$.

At this stage we recall that when S has values 0 and ∞ we have exact values for $h_2^\infty/h(c)$ and $h_1^\infty/(h(c)$ – see (2.38). It is therefore convenient to examine the asymptotics of (2.42) and (2.43) as $S \to 0$ and $S \to \infty$ respectively.

(i) limit as $S \to 0$:

$$\frac{h_2^\infty}{h(c)} = \tfrac{1}{2} + \tfrac{1}{2}S - S^{\alpha+1} - \tfrac{1}{2}S^{2\alpha} + \ldots, \tag{2.44}$$

$$\frac{h_1^\infty}{h(c)} = S^\alpha + \tfrac{1}{2}S^{2\alpha-1} + \ldots\,. \tag{2.45}$$

(ii) limit as $S \to \infty$:

$$\frac{h_2^\infty}{h(c)} = \frac{1}{S^\alpha} + \frac{1}{2S^{2\alpha-1}} - \frac{3}{2S^{2\alpha}} - \frac{1}{S^{3\alpha-1}} + \ldots, \tag{2.46}$$

$$\frac{h_1^\infty}{h(c)} = \frac{1}{2} + \frac{1}{2S} - \frac{1}{S^{\alpha+1}} - \frac{1}{2S^{2\alpha}} + \ldots\,. \tag{2.47}$$

From (2.38) we know that as $S \to 0$, $h_2^\infty/h(c) \to \frac{1}{2}$ and $h_1^\infty/h(c) \to 0$. Clearly from (2.45) it follows that $\alpha > \frac{1}{2}$. To be more specific we must appeal to some intuitive argument. One such argument is that as $S \to 0$ (and indeed when $S \to \infty$) then we might expect both h_1^∞ and h_2^∞ to exhibit the same asymptotic behaviour. Consequently (2.44) and (2.45) reveal that $\alpha = 1$, and ϕ is therefore given by

$$\phi = \frac{U_2}{U_2+U_1}. \tag{2.48}$$

Substituting for ϕ into (2.42) and (2.43), and recalling that

$$h(c) = H_0(1 + c^2/RH_0) \simeq 1{\cdot}226\,H_0,$$

yields the following algebraic expressions for the film-thickness ratios:

$$\lambda_1^{\mathrm{L}} = 0{\cdot}613\,\frac{S(S+3)}{(1+S)^2}, \tag{2.49}$$

$$\lambda_2^{\mathrm{L}} = 0{\cdot}613\,\frac{1+3S}{(1+S)^2}. \tag{2.50}$$

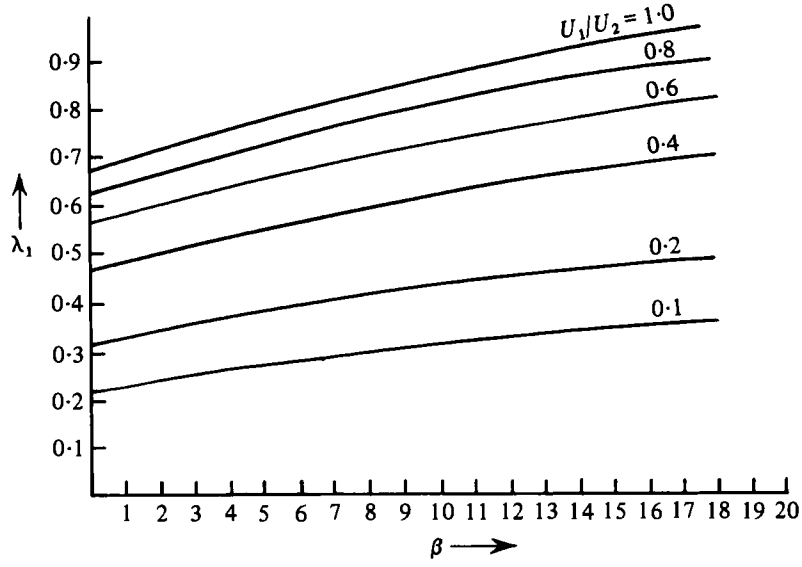

FIGURE 3. Variation of upper-film-thickness ratio λ_1 with modified capillary number, β, for speed ratios $U_1/U_2 = 0{\cdot}1$, $0{\cdot}2$, $0{\cdot}4$, $0{\cdot}6$, $0{\cdot}8$ and $1{\cdot}0$.

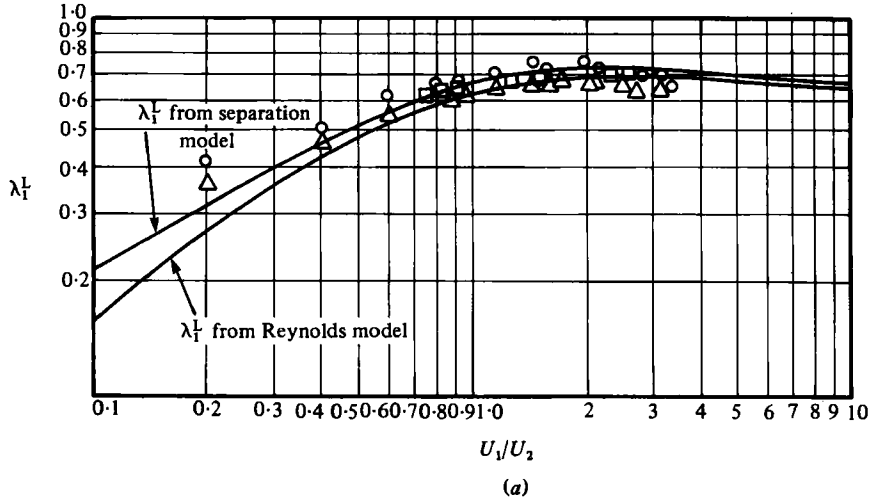

(*a*)

FIGURE 4. Variation of λ_1^L (*a*) and λ_2^L (*b*) with U_1/U_2 according to both the separation and Reynolds models, together with experimental data from Warren Spring laboratory: ○, △, □ refer to data obtained for gap thicknesses H_0 of 152, 272 and 600 μm respectively.

3. Mathematical solutions and discussions of results

For the separation model, a solution for λ_1 as a function of β and S follows from (2.25) and (2.26).

Step 1: specify speed ratio S, hence ϕ and ω are fixed.

Step 2: specify λ_1, hence C^* is fixed.

Step 3: evaluate the right-hand side of (2.26) either analytically or numerically, and hence β is determined.

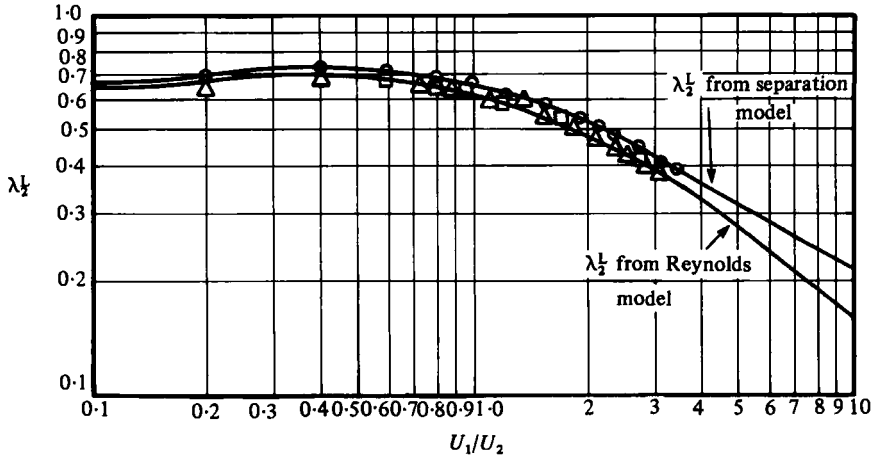

(*b*)

FIGURE 4(*b*). For legend see p. 452.

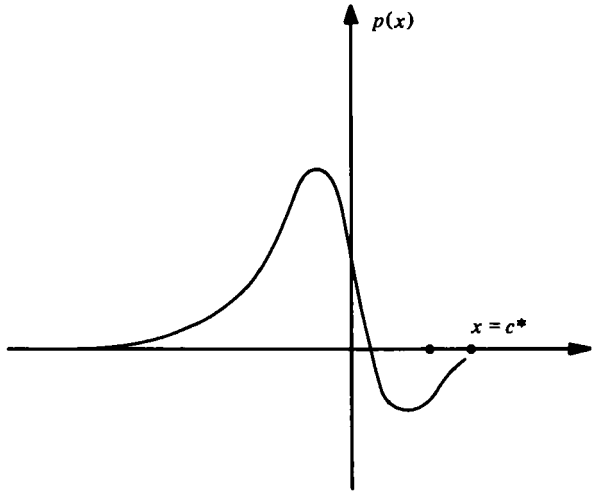

FIGURE 5. A typical pressure distribution from the separation model.

Figure 3 displays six graphs of λ_1 against β for six values of the speed ratio lying between 0·1 and 1·0. The variation of λ_1 and β is seen to be small for all S and β. Furthermore $H_0/R \ll 1$ is a necessary condition for lubrication theory to be valid and so in practice (where $T/\eta U$ is at most of order unity) β takes only small values, $0 < \beta \ll 1$. Hence if λ_1^L and λ_2^L are the limiting values of λ_1 and λ_2 such that $\lambda_1 \to \lambda_1^L$, $\lambda_2 \to \lambda_2^L$ as $\beta \to 0$, then it is appropriate to plot λ_1^L and λ_2^L. against S as shown in figures 4(*a*, *b*). They reveal that λ_1^L should start at zero when $S = 0$, rise to a value of $\frac{2}{3}$ when $S = 1$, reach a maximum when S is approximately 3·0, and then fall gradually to $\frac{2}{3}$ as S becomes large. Such trends are borne out in practice, as illustrated by the data from experiments performed on a roller rig at the Warren Spring Laboratory.

In the case of the Reynolds model the dependence of λ_1^L and λ_2^L on S is given by (2.49) and (2.50). Figure 4 shows a graph of λ_1^L that starts from zero with an initial

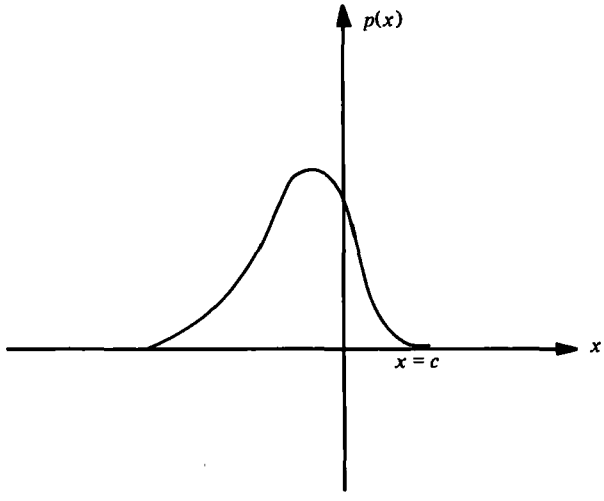

FIGURE 6. A typical pressure distribution from the Reynolds model.

Model	Range of application
Separation	$\beta > (T/H_0)\, p_A^{-1}$
Reynolds	$\beta < (T/H_0)\, p_A^{-1}, \quad \beta \ll 1$

TABLE 1.

slope of 1·83, reaches a maximum at $S = 3{\cdot}0$ and falls away gradually to a limit of 0·613 as S increases. In contrast, the variation of λ_2^L with S is shown in figure 5, where λ_2^L has an initial value of 0·613, reaches a maximum at $S = \frac{1}{3}$, and falls away to zero with increasing S. Clearly, agreement between theory and experiment compares equally well with that obtained using the separation model.

It may seem rather surprising that the two sets of theoretical predictions should be comparable, since both models cannot be simultaneously valid – their associated pressure distributions, figures 5 and 6, are quite distinct. Experiments on the roller rig were conducted under conditions in which the modified capillary number lay in the range $10^{-2} < \beta < 2{\cdot}10^{-1}$, whilst the ratio of surface tension to atmospheric pressure was in the range $10^{-3} < (T/H_0)\, P_A^{-1} < 10^{-2}$. Consequently, the criterion for using the separation model was always satisfied, $(T/H_0)\, \beta^{-1} < p_A$, and thus good agreement between theory and experiment is to be expected in this case.

Though β was small it was clearly not small enough for the generation of high fluid pressures. Therefore the Reynolds model does not provide an appropriate description of the pressure distributions attained in these experiments. However, though not qualitatively correct in the above sense, it does not seem to matter quantitatively, as far as the variation of λ_1^L and λ_2^L with S is concerned.

As a general statement to be drawn from this piece of research we may conclude that the separation model will be applicable to coating processes having β values in excess of $(T/H_0)\, p_A^{-1}$, and the Reynolds model will have application for β values smaller than $(T/H_0)\, p_A^{-1}$, provided, of course, that $\beta \ll 1$. This is summarized in table 1.

The work reported forms part of the project 'Transfer of Materials by Rollers', which is a component of the multiclient research programme 'Thick Liquids and Pastes: Processing and Flow', run by the Warren Spring Laboratory and funded jointly by the Department of Industry and a number of industrial companies.

REFERENCES

GREENER, Y. & MIDDLEMAN, S. 1975 *Polymer Engng & Sci.* **15**, 1.
HOPKINS, M. R. 1957 *Brit. J. Appl. Phys.* **8**, 442.
PEARSON, J. R. A. 1960 *J. Fluid Mech.* **7**, 481.
PITTS, E. & GREILLER, J. 1961 *J. Fluid Mech.* **11**, 33.
SAVAGE, M. D. 1977 *J. Fluid Mech.* **80**, 743.
SMITH, E. 1975 Ph.D. thesis, University of Leeds.